Performance Analysis of Alamouti Coded OFDM Systems over Wideband MIMO Car-to-Car Channels Correlated in Time and Space

Nurilla Avazov and Matthias Pätzold
Faculty of Engineering and Science, University of Agder
P.O. Box 509, NO-4898 Grimstad, Norway
E-mails: {nurilla.k.avazov, matthias.paetzold}@uia.no

Abstract — **In this paper, the performance of Alamouti coded orthogonal frequency division multiplexing (OFDM) systems over car-to-car (C2C) fading channels correlated in time and space is analyzed. Taking different geometrical scattering models into account, a generalized expression of the time-variant transfer function (TVTF) is derived for wideband multiple-input multiple-output (MIMO) C2C channels. We present a generalized expression for the bit error probability (BEP), which will be used to describe the performance of Alamouti coded OFDM systems over different types of C2C channel models, such as the rectangle model, the tunnel model, the street model, and the curve model. The effect of the maximum Doppler frequency and the antenna element spacing on the system performance is discussed. Furthermore, the proposed generalized model allows us to study the impact of the parameters of the geometrical model on the BEP. The proposed procedure enables us to investigate the system performance using different kinds of C2C fading channel models in a straightforward and time-efficient manner.**

I. Introduction

Over the past few decades, there has been an increased interest in studying and developing C2C communication systems, which offer numerous traffic safety applications to reduce the number of road accidents and to improve traffic flow. In this regard, a large number of research projects focusing on C2C communication systems have been carried out in Europe [1–3].

The development of C2C communication systems highly depends on a detailed knowledge of the underlying radio channel. In the literature, numerous C2C channel models have been developed and analyzed, such as the street line model [4], the rectangle model [5], the cross-junction model [6], the curve model [7], and the tunnel model [8]. The time-frequency selective properties of C2C channels are significantly different from those of traditional fixed-to-mobile or mobile-to-fixed

channels. Using OFDM systems can be of great advantage for C2C communications due to their high spectral efficiency and their ability to mitigate multipath fading effects.

In [9, 10], the performance of car-to-infrastructure (C2I) communication systems is analyzed. The frame success ratios and goodputs of C2I channels in a tunnel environment were discussed and analyzed in [9], where it was shown that the use of higher-order modulation schemes with constant packet length is more beneficial to the total goodput than an increase in packet length. In [10], a narrowband single-input single-output (SISO) C2I channel model for blind bent environments has been derived. The authors of [10] studied the performance of different digital modulation schemes over channels modelled by a sum of singly and doubly scattered components. A computationally low-cost packet error model has been proposed for C2I communications in [11], where the performance influence of different system configurations and components were analyzed jointly.

The performance of C2C communication systems was analyzed in [12, 13]. The impact of fast-varying channels on the C2C system performance was studied in [12]. It was shown that the channel estimation process is the most affected part due to the rapid changes of the channel. In [13], the performance evaluation of the long term evolution (LTE) technology in a C2C communication system was conducted. The obtained results in [13] show the feasibility of broadband wireless access at data rates of several Mbit/s. Another, recently published work dealing with the performance analysis of C2C communications can be found in [14], where a new regular shaped geometry-based stochastic model for non-isotropic scattering wideband C2C Rician fading channels has been proposed. There, to combat intercarrier interference (ICI), the authors proposed a new ICI cancellation scheme, called precoding-based cancellation (PBC) scheme. Real-world measurement-based performance results of C2C communications in various road configurations under varying LOS conditions were presented in [15]. There, the effect of objects blocking the LOS path on the range of C2C communications was analyzed. Tapped delay line C2C channel models have been designed in [16] based on the bit error rate (BER) performance.

To the best of the authors' knowledge, a theoretical analysis of the performance of C2C communication systems over C2C channels under different scattering conditions, as described in [4–8] has not been performed yet. Therefore, to fill this gap, we have analyzed the performance of an Alamouti coded [17] OFDM system over different C2C channel models, such as the rectangle model [5], the tunnel model [8], the street line model [4], and the curve model [7].

The main contributions and novelties of this paper are as follows:

1) We combine all abovementioned channel models [4, 5, 7, 8] to a generalized wideband MIMO C2C channel model assuming single-bounce scattering. The proposed model includes as special cases the rectangle model, the tunnel model, the street line model, and the curve model.

2) We extend the wideband SISO C2C tunnel model in [8] to a MIMO C2C tunnel channel model.

3) We also provide an extension of the narrowband MIMO C2C curve model towards frequency selectivity.

4) Furthermore, we represent the corresponding correlation functions of the proposed generalized model, such as the two-dimensional (2D) space cross-correlation function (CCF) and the temporal autocorrelation function (ACF).

5) Finally, a comparative study of the BEP of Alamouti coded OFDM systems is presented by using all abovementioned channel models [4, 5, 7, 8].

The rest of this paper is organized as follows. Section II describes the generalized reference model. In Section III, the correlation functions of the reference channel model, such as the 2D space CCF and the temporal ACF are briefly described. Analytical expressions for the BEP of Alamouti coded OFDM systems are presented in Section IV. The illustration of the numerical results found for the BEP is the topic of Section V. Finally, Section VI provides the conclusions of the paper.

II. A Generalized Wideband MIMO C2C Channel Model

In this section, we present a generalized reference channel model for a wideband MIMO C2C channel assuming single-bounce scattering. The proposed generalized reference channel model can be used to describe the geometrical rectangle model and the tunnel model, as well as the street line model and the curve model as a special case. The reference model is obtained by assuming that the number of scatterers is infinite. The reference model serves as a basis for the derivation of efficient MIMO channel simulators. In our proposed generalized channel model, we consider two models, i.e., the rectangle model and the tunnel model, where the positions of the scatterers $S^{(mn)}$ for $m = 1,2,\ldots,M$ and $n = 1,2,\ldots,N$ are described as shown in [5, Fig. 2] and [8, Fig. 3], respectively. In both models, Cartesian coordinates (x_m, y_n) are used to desribe the positions of the scatterers $S^{(mn)}$, where x_m and y_n are random variables. The distribution of the scatterers $S^{(mn)}$ is completely

determined by the distributions of x_m and y_n. In the following, we use the notation and the definitions of the model parameters in [5, Fig. 2] and [8, Fig. 3], which are summarized in Table E.1.

Table E.1: Definition of the parameters used in [5, Fig. 2] and [8, Fig. 3].

L	The length of the tunnel.
R	The radius of the semicircle tunnel.
(x_T, y_T, z_T)	The position of the mobile transmitter (MS_T).
(x_R, y_R, z_R)	The position of the mobile receiver (MS_R).
D	The distance between the MS_T and the MS_R.
$L_A = A_1 + A_2$	The length of the rectangular grids.
B_1, B_2	The width of the rectangular grids.
y_{T_1} (y_{R_1})	The distance from the left-hand side of the street to the MS_T (MS_R).
y_{T_2} (y_{R_2})	The distance from the right-hand side of the street to the MS_T (MS_R).
γ_T (γ_R)	The orientation of the transmitter (receiver) antenna array in the xy-plane relative to the x-axis.
ϕ_T (ϕ_R)	The elevation angle of the transmitter (receiver) antenna array w.r.t. the xy-plane.
δ_T (δ_R)	The spacing between the antenna elements at the transmitter (receiver) antenna.
v_T (v_R)	The speed of the mobile transmitter (receiver).
φ_{v}^T (φ_{v}^R)	The angle of motion of the MS_T (MS_R).
$\alpha_T^{(mn)}$, $\alpha_R^{(mn)}$	The azimuth angle of departure (AAOD) and the azimuth angle of arrival (AAOA).
$\beta_T^{(mn)}$, $\beta_R^{(mn)}$	The elevation angle of departure (EAOD) and the elevation angle of arrival (EAOA).
$D_T^{(l,mn)}$, $D_R^{(mn,k)}$, $D_{TR}^{(l,k)}$,	The Euclidean distances $d\left(A_T^{(l)}, S^{(mn)}\right)$, $d\left(S^{(mn)}, A_R^{(k)}\right)$, and $d\left(A_T^{(l)}, A_R^{(k)}\right)$.

A. A Generalized TVTF

Let us assume a wideband MIMO C2C communication system employing M_T transmitter antennas and M_R receiver antennas. The wideband MIMO C2C channel can be described by the channel matrix $\mathbf{H}_p(f',t) = [H_{kl,p}(f',t)]_{M_R \times M_T}$, where

$H_{kl,p}(f',t)$ denotes the TVTF of the link from the lth transmitter antenna $A_T^{(l)}$ ($l = 1,2,\ldots,M_T$) to the kth receiver antenna $A_R^{(k)}$ ($k = 1,2,\ldots,M_R$), and the index p indicates the type of the geometrical channel model. We consider a rectangle model if $p = 1$ and a tunnel model if $p = 2$. The TVTF $H_{kl,p}(f',t)$ of the pth channel model for the link $A_T^{(l)} - A_R^{(k)}$ can be expressed as

$$H_{kl,p}(f',t) = \lim_{\substack{M\to\infty \\ N\to\infty}} \frac{1}{\sqrt{MN}} \sum_{m,n=1}^{M,N} e^{-j\frac{2\pi}{\lambda}D_{kl,p}^{(mn)}} e^{j\left[2\pi f_p^{(mn)}t + \theta^{(mn)} - 2\pi\tau_{kl,p}^{\prime(mn)}f'\right]} \quad \text{(E.1)}$$

where

$$D_{kl,p}^{(mn)} = D_{T,p}^{(l,mn)} + D_{R,p}^{(mn,k)},\ p \in \{1,2\} \quad \text{(E.2)}$$

$$f_p^{(mn)} = f_{T,p}^{(mn)} + f_{R,p}^{(mn)},\ p \in \{1,2\} \quad \text{(E.3)}$$

$$f_{T,p}^{(mn)} = f_{T_{\max}} \cos\left(\alpha_{T,p}^{(mn)} - \varphi_{\mathrm{v}}^{T}\right) \cos\left((p-1)\beta_T^{(mn)}\right) \quad \text{(E.4)}$$

$$f_{R,p}^{(mn)} = f_{R_{\max}} \cos\left(\alpha_{R,p}^{(mn)} - \varphi_{\mathrm{v}}^{R}\right) \cos\left((p-1)\beta_R^{(mn)}\right). \quad \text{(E.5)}$$

The symbols $D_{kl.p}^{(mn)}$, $f_p^{(mn)}$, $\theta^{(mn)}$, and $\tau_{kl,p}^{\prime(mn)}$ in (E.1) denote the total path length, the Doppler frequency, the phase, and the propagation delay of the reference model. The distance $D_{kl,p}^{(mn)}$ is determined by (E.2) in which the distances $D_{T,p}^{(l,mn)}$ and $D_{R,p}^{(mn,k)}$ are given by

$$\begin{aligned} D_{T,p}^{(l,mn)} = {} & D_{T,p}^{(mn)} - (M_T - 2l + 1)\frac{\delta_T}{2}\left[\cos\left((p-1)\phi_T\right)\cos\left((p-1)\beta_T^{(mn)}\right)\right. \\ & \left.\cdot\cos\left(\gamma_T - \alpha_{T,p}^{(mn)}\right) + (p-1)\sin\left(\phi_T\right)\sin\left(\beta_T^{(mn)}\right)\right],\ p \in \{1,2\} \end{aligned} \quad \text{(E.6)}$$

$$\begin{aligned} D_{R,p}^{(mn,k)} = {} & D_{R,p}^{(mn)} - (M_R - 2k + 1)\frac{\delta_R}{2}\left[\cos\left((p-1)\phi_R\right)\cos\left((p-1)\beta_R^{(mn)}\right)\right. \\ & \left.\cdot\cos\left(\gamma_R - \alpha_{R,p}^{(mn)}\right) + (p-1)\sin\left(\phi_R\right)\sin\left(\beta_R^{(mn)}\right)\right],\ p \in \{1,2\} \end{aligned} \quad \text{(E.7)}$$

respectively, where

$$D_{T,p}^{(mn)} = \left[(x_m - (p-1)x_T)^2 + (y_n - (p-1)y_T)^2 + (p-1)(\sqrt{R^2 - y_n^2} - z_T)^2\right]^{\frac{1}{2}} \quad \text{(E.8)}$$

$$\begin{aligned} D_{R,p}^{(mn)} = {} & \left[(x_m - (p-1)x_R + (p-2)D_x)^2 + (y_n - (p-1)y_R + (p-2)D_y)^2\right. \\ & \left. + (p-1)(\sqrt{R^2 - y_n^2} - z_R)^2\right]^{\frac{1}{2}}. \end{aligned} \quad \text{(E.9)}$$

The symbols D_x and D_y in (E.9) are defined as $D_x = D$ and $D_y = y_{T_1} - y_{R_1}$, respectively (see [5, Fig. 2]). It is assumed that the phases $\theta^{(mn)}$ are independent, identically distributed (i.i.d.) random variables, which are uniformly distributed over the interval $[0, 2\pi)$. Using the distance $D_{kl,p}^{(mn)}$ in (E.2), the propagation delays $\tau_{kl,p}^{\prime(mn)}$ in (E.1) can be computed as $\tau_{kl,p}^{\prime(mn)} = D_{kl,p}^{(mn)}/c_0$, where c_0 is the speed of light. It is noteworthy that we have extended in this paper the SISO C2C semicircle tunnel model in [8] to a MIMO model.

The proposed generalized channel model also includes the street line model ($p = 3$) and the curve model ($p = 4$) as special cases. In these models, it is assumed that an infinite number of scatterers are uniformly distributed on a street line (street line model) [4] or on a curve (curve model) [7]. Hence, the double-sum in (E.1) will be reduced to a single-sum, i.e., $N = 1$, by only taking into account the effect of the scatterers $S^{(m)}$. Thus, the TVTF $H_{kl,p}(f',t)$ of the reference model can be represented as

$$H_{kl,p}(f',t) \;=\; \lim_{M\to\infty} \frac{1}{\sqrt{M}} \sum_{m=1}^{M} e^{-j\frac{2\pi}{\lambda} D_{kl,p}^{(m)}} e^{j\left[2\pi f_p^{(m)} t + \theta^{(m)} - 2\pi\tau_{kl,p}^{\prime(m)} f'\right]} \qquad \text{(E.10)}$$

where

$$D_{kl,p}^{(m)} \;=\; D_{T,p}^{(l,m)} + D_{R,p}^{(m,k)},\; p \in \{3,4\} \qquad \text{(E.11)}$$

$$D_{T,p}^{(l,m)} = D_{T,p}^{(m)} - (M_T - 2l + 1)\frac{\delta_T}{2}\cos\left(\alpha_{T,p}^{(m)} - \gamma_T\right) \qquad \text{(E.12)}$$

$$D_{R,p}^{(m,k)} = D_{R,p}^{(m)} - (M_R - 2k + 1)\frac{\delta_R}{2}\cos\left(\alpha_{R,p}^{(m)} - \gamma_R\right) \qquad \text{(E.13)}$$

$$f_p^{(m)} \;=\; f_{T,p}^{(m)} + f_{R,p}^{(m)},\; p \in \{3,4\} \qquad \text{(E.14)}$$

$$f_{T,p}^{(m)} \;=\; f_{T_{\max}} \cos\left(\alpha_{T,p}^{(m)} - \varphi_{\mathrm{v}}^{T}\right) \qquad \text{(E.15)}$$

$$f_{R,p}^{(m)} \;=\; f_{R_{\max}} \cos\left(\alpha_{R,p}^{(m)} - \varphi_{\mathrm{v}}^{R}\right). \qquad \text{(E.16)}$$

The symbols $D_{T,p}^{(m)}$ and $D_{R,p}^{(m)}$ in (E.12) and (E.13), respectively, can be found in [4] for $p = 3$ and in [7] if $p = 4$, respectively.

B. Angle of Departure (AOD) and Angle of Arrival (AOA)

In the generalized reference model, the positions of all scatterers $S^{(mn)}$ are described by the Cartesian coordinates (x_m, y_n) if $p \in \{1,2\}$. For the special cases $p \in \{3,4\}$, the position of each scatterer is defined by the AOD and/or the angle of scatterer (AOS). Thus, the angles $\alpha_{T,p}^{(mn)}$ ($\alpha_{R,p}^{(mn)}$) [see (E.4) and (E.5)] and $\alpha_{T,p}^{(m)}$ ($\alpha_{R,p}^{(m)}$) [see (E.15) and (E.16)] are listed in Table E.2. According to [8, Eq. (15)],

Table E.2: AODs and AOAs of the reference model

Geometrical Model	**AOD**	**AOA**
Rectangle Model ($p=1$)	$\alpha_{T,1}^{(mn)}$ given in [5, Eq. (16)]	$\alpha_{R,1}^{(mn)}$ given in [5, Eq. (17)]
Tunnel Model ($p=2$)	$\alpha_{T,2}^{(mn)}$ given in [8, Eq. (15)]	$\alpha_{R,2}^{(mn)}$ given in [8, Eq. (15)]
Street Line Model ($p=3$)	$\alpha_{T,3}^{(m)}$ given in [4]	$\alpha_{R,3}^{(m)}$ given in [4, Eq. (14)]
Curve Model ($p=4$)	$\alpha_{T,4}^{(m)}$ given in [7, Eq. (24)]	$\alpha_{R,4}^{(m)}$ given in [7, Eq. (25)]

the EAOD $\beta_T^{(mn)}$ and the EAOA $\beta_R^{(mn)}$ can be expressed in terms of the coordinates of the position (x_m, y_n) of the scatterer $S^{(mn)}$. In the curved street scattering model, the position of the scatterer $S^{(m)}$ is described by the AOS $\beta^{(m)}$. Hence, for $p=4$, the angle $\alpha_{T,4}^{(m)}$ ($\alpha_{R,4}^{(m)}$) is defined in terms of the AOS as given in [7, Eq. (24)-(25)].

III. Correlation Properties of the Reference Model

In [18], it was shown that the performance of Alamouti coded OFDM systems depends on the temporal and spatial correlation properties of the underlying channel. In this regard, we will briefly review the main correlation functions, such as the 2D space CCF and the temporal ACF.

Starting from the derivation of the analytical expression for the space-time-frequency CCF (STF-CCF) of the Type p C2C (C2C$_p$) channel model, we will compute the corresponding 2D space CCF and the temporal ACF. The STF-CCF of the TVTFs $H_{kl,p}(f',t)$ and $H_{k'l',p}(f',t)$ is defined as $\rho_{kl,k'l',p}(\delta_T,\delta_R,\nu',\tau) := E\{H_{kl,p}^*(f',t)H_{k'l',p}(f'+\nu',t+\tau)\}$. From the STF-CCF, we can obtain the 2D space CCF $\rho_{kl,k'l',p}(\delta_T,\delta_R)$ of the reference model by setting $\tau=0$ and $\nu'=0$. The 2D space CCF for $p=1$, $p=3$, and $p=4$ can be found in [5, Eq. (30)], [4, Eq. (27)], and [7, Eq. (47)], respectively. The 2D space CCF $\rho_{kl,k'l',p}(\delta_T,\delta_R)$ of the reference model for $p=2$, i.e., for the tunnel model, can be expressed as

$$\rho_{kl,k'l',2}(\delta_T,\delta_R) = \int_{-R}^{R}\int_{x_T}^{x_R} p_{x_m y_n}(x,y)c_{ll'}(x,y)d_{kk'}(x,y)dxdy \tag{E.17}$$

where

$$\begin{aligned} c_{ll'}(x,y) &= e^{j2\pi\frac{\delta_T}{\lambda}(l-l')\cos\phi_T\cos(\beta_T(x,y))\cos(\gamma_T-\alpha_T(x,y))} \\ &\quad \cdot e^{j2\pi\frac{\delta_T}{\lambda}\sin\phi_T\sin(\beta_T(x,y))} \end{aligned} \tag{E.18}$$

$$\begin{aligned} d_{kk'}(x,y) &= e^{j2\pi\frac{\delta_R}{\lambda}(k-k')\cos\phi_R\cos(\beta_R(x,y))\cos(\gamma_R-\alpha_R(x,y))} \\ &\quad \cdot e^{j2\pi\frac{\delta_R}{\lambda}\sin\phi_R\sin(\beta_R(x,y))} \end{aligned} \tag{E.19}$$

and $p_{x_m y_n}(x,y)$ denotes the joint probability density function of the random variables x_m and y_n [8, Eq. (23)].

The temporal ACF $r_{kl,p}(\tau)$ of the TVTF of the transmission link $A_T^{(l)} - A_R^{(k)}$ is defined by $r_{kl,p}(\tau) := E\{H_{kl,p}^*(f',t)H_{kl,p}(f',t+\tau)\}$ [19, p. 376]. By making use of the results in [5, Eq. (32)], [8, Eq. (32)], [4, Eq. (26)], and [7, Eq. (48)], the temporal ACF $r_{kl,p}(\tau)$ can be expressed for all considered C2C$_p$ channel models.

IV. BEP of Alamouti Coded OFDM Systems

In this section, we present the expression of the BEP for Alamouti coded OFDM systems over C2C$_p$ channels correlated in time and space. The BEP of Alamouti coded OFDM systems can be computed as

$$P_b = \int_0^\infty P_{\gamma_\Sigma}(\gamma)\cdot P_{b|\gamma_\Sigma}(\gamma)d\gamma \tag{E.20}$$

where $P_{\gamma_\Sigma}(\gamma)$ denotes the joint PDF given by [18, Eq. (24)], and $P_{b|\gamma_\Sigma}(\gamma)$ is the conditional BEP of a digital modulation scheme for a given value of the signal-to-noise ratio (SNR) γ. For example, for the binary phase-shift keying (BPSK) modulation scheme, the conditional BEP equals $P_{b|\gamma_\Sigma}(\gamma) = \operatorname{erfc}\left(\sqrt{\gamma}\right)/2$.

Under the assumption of perfect channel state information (CSI), the BEP $P_{b,p}$ of BPSK Alamouti coded OFDM systems over C2C$_p$ channels correlated in time can be written as [18, Eq. (27)]

$$\begin{aligned} P_{b,p} &= \frac{2\sigma_0^2}{16(\sigma_0^4-\rho_{T,p}^2)^2\bar{\gamma}}\int_0^\infty\int_0^\infty\int_0^w\int_0^{z_2}\frac{z_2 z_3(w-z_3)}{z_4(z_2-z_4)w} \\ &\quad \cdot e^{-\frac{\sigma_0^2}{2(\sigma_0^4-\rho_{T,p}^2)}\left[\frac{(w-z_3)^2}{z_4}+z_2+\frac{z_3^2}{z_2-z_4}\right]}\operatorname{erfc}(\sqrt{\gamma}) \\ &\quad \cdot I_0\left(\frac{z_3\rho_{T,p}}{\sigma_0^4-\rho_{T,p}^2}\right)I_0\left(\frac{(w-z_3)\rho_{T,p}}{\sigma_0^4-\rho_{T,p}^2}\right)dz_4dz_3dz_2d\gamma \end{aligned} \tag{E.21}$$

where σ_0^2 is one half of the mean power of the received scattered components, the upper limit w is given by $w = \sqrt{2\sigma_0^2\gamma z_2/\bar{\gamma}}$, and $\rho_{T,p} = r_{kl,p}(T_s)/2$, where T_s is the symbol duration.

In an analogous manner, the BEP $P_{b,p}$ of a BPSK Alamouti coded OFDM system over C2C$_p$ channels correlated in space can be expressed as [18, Eq. (28)]

$$\begin{aligned} P_{b,p} \;=\; & \frac{2\sigma_0^2}{16(\sigma_0^4-\rho_{\Delta,p}^2)^2\bar{\gamma}} \int_0^{\infty}\int_0^{\infty}\int_0^{w}\int_0^{z_2} \frac{z_2 z_3 (w-z_3)}{z_4(z_2-z_4)w} \\ & \cdot e^{-\frac{\sigma_0^2}{2(\sigma_0^4-\rho_{\Delta,p}^2)}\left[\frac{(w-z_3)^2}{z_4}+z_2+\frac{z_3^2}{z_2-z_4}\right]} \operatorname{erfc}\left(\sqrt{\gamma}\right) \\ & \cdot I_0\left(\frac{z_3\sqrt{z_4}\rho_{\Delta,p}}{(\sigma_0^4-\rho_{\Delta,p}^2)\sqrt{z_2-z_4}}\right) \\ & \cdot I_0\left(\frac{(w-z_3)\sqrt{z_2-z_4}\rho_{T,p}}{(\sigma_0^4-\rho_{T,p}^2)\sqrt{z_4}}\right) dz_4 dz_3 dz_2 d\gamma \end{aligned} \tag{E.22}$$

where $\rho_{\Delta,p} = \rho_{kl,k'l',p}(\delta_T, 0)/2$.

V. Performance Analysis

This section presents the theoretical BEP results obtained by evaluating (E.21) and (E.22). The correctness of the analytical results will be confirmed by system simulations. For the system simulations, we consider an OFDM system with $K = 64$ subcarriers and $T_s = 8\mu s$. The geometrical model parameters used for computing the BEP in (E.21) and (E.22) are presented in Table E.3. For the reference model, all numerical results have been obtained by choosing the following parameters: $\varphi_{\mathrm{v}}^T =$

Table E.3: Model parameters.

Model parameters	Value and unit
R	5 m
(x_T, y_T, z_T)	(20 m, 2 m, 1 m)
(x_R, y_R, z_R)	(40 m, 2 m, 1 m)
D	400 m [5]
$L_A = A_1 + A_2$	500 m [5]
B_1, B_2	100 m
y_{T_1} (y_{R_1})	20 m (10 m)
y_{T_2} (y_{R_2})	10 m (20 m)

$\varphi_{\mathrm{v}}^{R}=0^{\circ}$, $\phi_T=\phi_R=45^{\circ}$, $\gamma_T=\gamma_R=45^{\circ}$, and $f_{T_{\max}}=f_{R_{\max}}=100\,\mathrm{Hz}$. The corresponding MIMO channel simulator has been designed by using the L_p-norm method, such that the resulting simulation model is ergodic [20], i.e., the statistical average equals the time average. This allows us to compute the BEP from single runs. For each single run, we have generated 10^6 data symbols.

In Fig. E.1, the BEP of an Alamouti coded OFDM system over different C2C fading channels correlated in time versus the SNR has been illustrated. In our analysis, as mentioned in Section IV, it has been assumed that the CSI is known at the receiver side. Hence, from Fig. E.1, we can conclude that the maximum Doppler frequency $f_{T_{\max}}$ ($f_{R_{\max}}$) does not affect the system performance if $f_{T_{\max}}$ ($f_{R_{\max}}$) changes over the range from 100 Hz to 500 Hz. It is worth mentioning that all considered C2C channels behave in the same manner, as the same BEP is demonstrated. Moreover, it should be mentioned that the system simulation results match those of the theoretical BEPs.

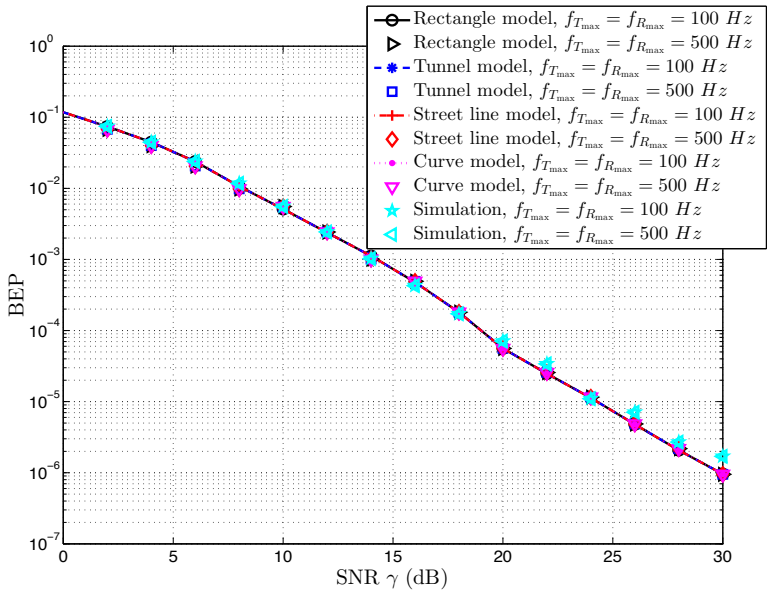

Figure E.1: BEP performance of an Alamouti coded OFDM system over different C2C fading channels correlated in time.

Figure E.2 shows the BEP performance over different C2C fading channels correlated in space for $\delta_T=0.1\lambda$ and $\delta_T=3\lambda$. From this figure, we can conclude that the system performance can be improved by increasing the antenna spacings. This fact indicates that the spatial correlation between TVTFs $H_{kl,p}(f',t)$ and $H_{k'l',p}(f',t)$ is smaller if the antenna element spacings are large. Similarly to Fig. E.1, the curves obtained for the BEP are approximately the same for different C2C channel models.

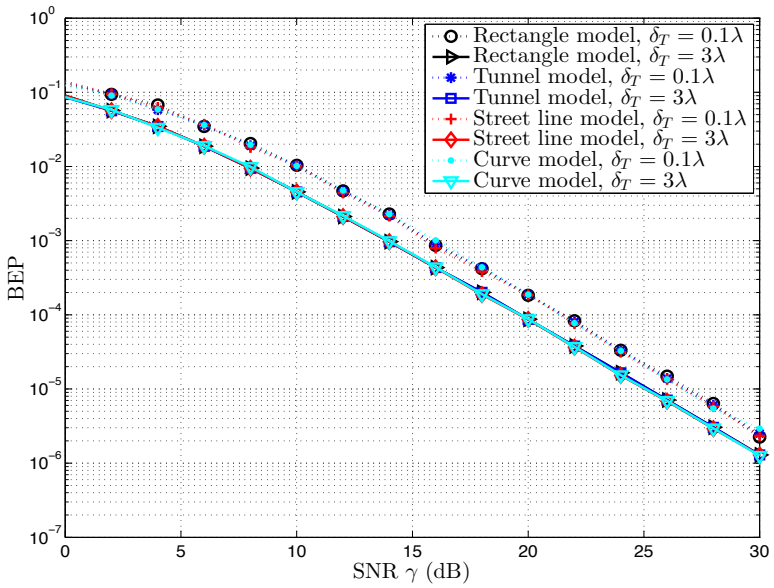

Figure E.2: BEP performance of an Alamouti coded OFDM system over different C2C fading channels correlated in space with $\delta_T = 0.1\lambda$ and $\delta_T = 3\lambda$.

Figure E.3 shows the effect of the street length L_A and the distance D between MS_T and MS_R on the BEP performance. The system performance improves as the length of the street L_A increases. However, the BEP performance does not change for different values of the distance between MS_T and MS_R. The change of the street width B_1 and B_2 does not affect the BEP performance, which can be seen in Fig. E.4. This fact can be attributed to the presence of a large number of scatterers located on a street line. Nevertheless, the system performance can be improved by increasing antenna spacings δ_T from 0.1λ to 3λ.

The effect of the tunnel model parameters, i.e., the radius R of the tunnel arch and the distance D between MS_T and MS_R, on the performance of C2C communication systems has been demonstrated for different antenna element spacings δ_T in Fig. E.5. We can see the same performance in terms of the BEP for different values of R and D, which means that small changes in R and D do not affect the system performance. From Fig. E.5, one can see the effect of the antenna spacings δ_T, in which the system performance is improved by increasing δ_T.

Finally in Fig. E.6, the system performance of the C2C channel model based on the curve model is shown. Similarly to Fig. E.5, the BEP performance does not change if the radius R of the curve varies in the considered range.

VI. Conclusion

In this paper, a generalized reference model for wideband MIMO C2C channels has been derived by assuming single-bounce scattering. An extension from the

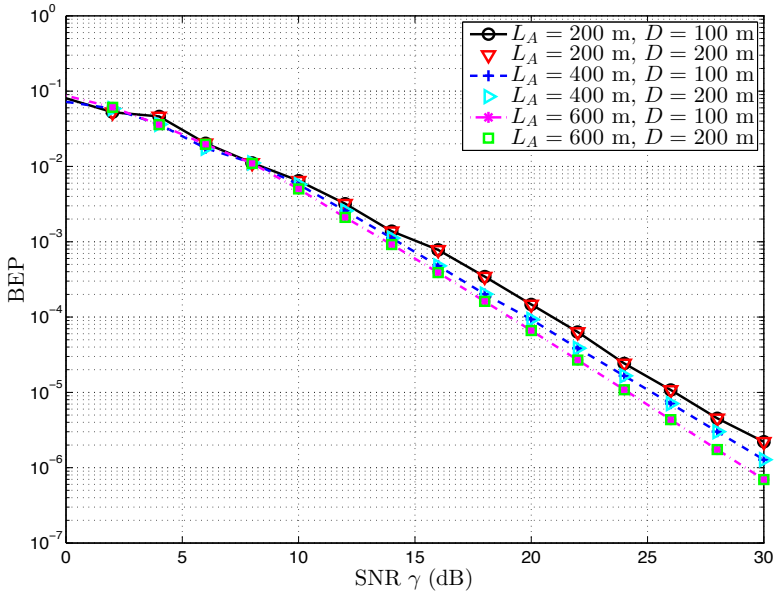

Figure E.3: BEP performance of an Alamouti coded OFDM system over a C2C channel (rectangle model) for different values of L_A and D.

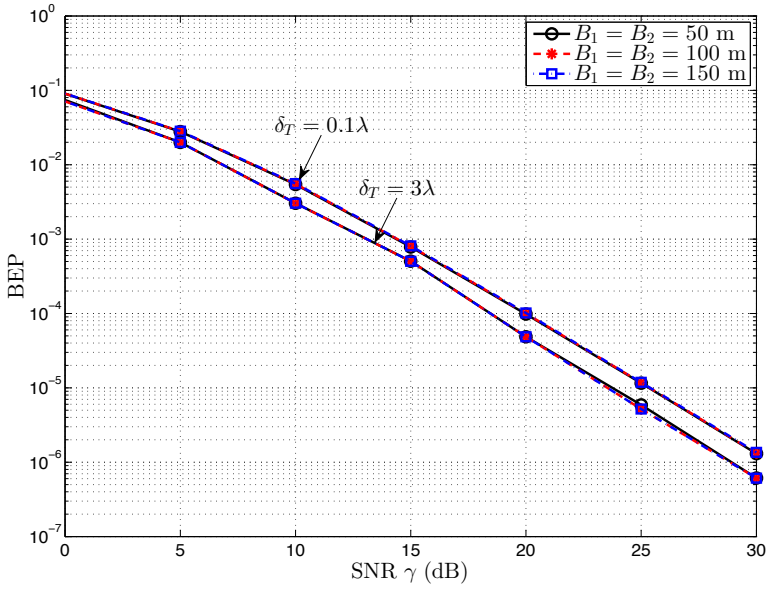

Figure E.4: BEP performance of an Alamouti coded OFDM system over a C2C channel (rectangle model) for different values of B_1 and B_2.

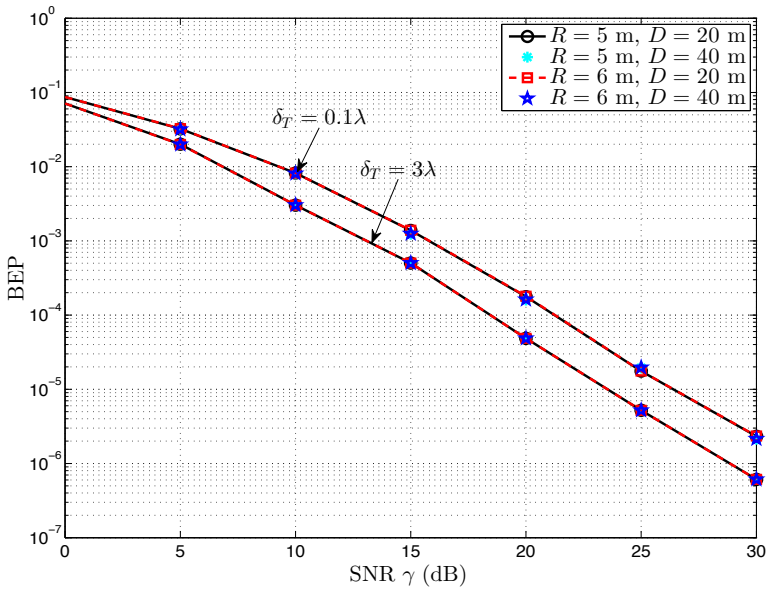

Figure E.5: BEP performance of an Alamouti coded OFDM system over a C2C channel (tunnel model) for different values of R and D.

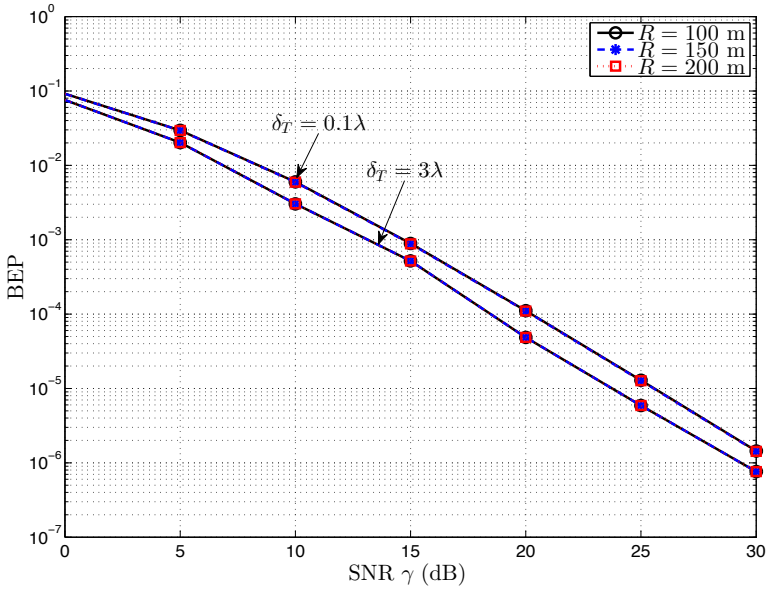

Figure E.6: BEP performance of an Alamouti coded OFDM system over a C2C channel (curve model) for different values of the curve radius R.

SISO C2C tunnel model to the MIMO case has been performed. Furthermore, an extension of the narrowband MIMO C2C channel model based on the curve model to the wideband model has been provided. An analytical expression has been presented for the BEP of Alamouti coded OFDM systems over generalized C2C channels. The effect of the geometrical model parameters of the propagation area on the system performance has been studied and discussed. It has been shown that using large antenna element spacings improves the system performance. The proposed generalized C2C channel model can serve as a highly flexible C2C channel simulator, which allows system developers to simulate a variety of C2C channels and to evaluate their performance under different propagation conditions.

REFERENCES

[1] G. Rafiq, B. Talha, M. Pätzold, J. G. Luis, G. Ripa, I. Carreras, C. Coviello, S. Marzorati, G. P. Rodrigues, G. Herrero, and M. Desaeger, "What's new in intelligent transportation systems? An overview of European projects and initiatives," *IEEE Veh. Technol. Mag.*, vol. 8, no. 4, pp. 45–69, Dec. 2013.

[2] Car-to-Car Communication Consortium (C2C-CC) [Online]. Available: http://www.car-to-car.org.

[3] European Road Transport Telematics Implementation Coordinating Organization (ERTICO) [Online]. Available: http://www.ertico.com.

[4] A. Chelli and M. Pätzold, "A MIMO mobile-to-mobile channel model derived from a geometric street scattering model," in *Proc. 4th IEEE International Symposium on Wireless Communication Systems, ISWCS 2007, Trondheim, Norway*, Oct. 2007, pp. 792–797.

[5] N. Avazov and M. Pätzold, "Design of wideband MIMO car-to-car channel models based on the geometrical street scattering model," *Special Issue: Modelling and Simulation in Engineering*, vol. 2012, Sept. 2012.

[6] A. Theodorakopoulos, P. Papaioannou, T. Abbas, and F. Tufvesson, "A geometry based stochastic model for MIMO V2V channel simulation in cross-junction scenario," in *Proc. 13th International Conference on ITS Telecommunications, Tampere, Finland*, Nov. 2013, pp. 290–295.

[7] N. Avazov and M. Pätzold, "A novel MIMO car-to-car channel model based on the geometrical curved street scattering model," in *Proc. Loughborough An-*

tennas and Propagation Conference, LAPC'2012, Loughborough, UK, Nov. 2012, pp. 1–6.

[8] ——, "A wideband car-to-car channel model based on a geometrical semi-circular tunnel scattering model," in *Proc. 24th IEEE Int. Symp. on Personal, Indoor and Mobile Radio Communications, PIMRC 2013, London, UK*, Sept. 2013, pp. 253–258.

[9] V. Shivaldova, G. Maier, D. Smely, N. Czink, A. Alonso, A. Winkelbauer, A. Paier, and C. F. Mecklenbräuker, "Performance evaluation of IEEE 802.11p infrastructure-to-vehicle tunnel measurements," in *Proc. 7th International Wireless Communications and Mobile Computing Conference, IWCMC 2011, Istanbul, Turkey*, Jul. 2011, pp. 848–852.

[10] A. Chelli, R. Hamdi, and M.-S. Alouini, "Channel modelling and performance analysis of V2I communication systems in blind bend scattering environments," *Progress in Electromagnetics Research B*, vol. 57, pp. 233–251, 2014.

[11] V. Shivaldova, A. Winkelbauer, and C. F. Mecklenbräuker, "Vehicular link performance: From real-world experiments to reliability models and performance analysis," *IEEE Veh. Technol. Mag.*, vol. 8, no. 4, pp. 35–44, Dec. 2013.

[12] I. Ivan, P. Besnier, M. Crussiere, M. Drissi, L. Le Danvic, M. Huard, and E. Lardjane, "Physical layer performance analysis of V2V communications in high velocity context," in *Proc. 9th International Conference on Intelligent Transport Systems Telecommunications, ITST 2009, Lille, France*, Oct. 2009, pp. 409–414.

[13] D. W. Matolak, W. Qiong, J. J. Sanchez-Sanchez, D. Morales-Jimenez, and M. C. Aguayo-Torres, "Performance of LTE in vehicle-to-vehicle channels," in *Proc. IEEE Vehicular Technology Conference, VTC2011-Fall, San Francisco, CA*, Sept. 2011, pp. 1–4.

[14] X. Cheng, Q. Yao, M. Wen, C.-X. Wang, L.-Y. Song, and B.-L. Jiao, "Wideband channel modeling and intercarrier interference cancellation for vehicle-to-vehicle communication systems," *IEEE J. Select. Areas Commun.*, vol. 31, no. 9, pp. 434–448, Sept. 2013.

[15] A. Böhm, K. Lidström, M. Jonsson, and T. Larsson, "Evaluating CALM M5-based vehicle-to-vehicle communication in various road settings through field

trials," in *Proc. 35th IEEE Conference on Local Computer Networks (LCN)*, Oct. 2010, pp. 613–620.

[16] G. Acosta-Marum and M. A. Ingram, "A BER-based partitioned model for a 2.4 GHz vehicle-to-vehicle expressway channel," *Wireless Personal Communications (WPC)*, vol. 37, pp. 421–443, 2006.

[17] S. M. Alamouti, "A simple transmit diversity technique for wireless communications," *IEEE J. Select. Areas Commun.*, vol. 16, no. 8, pp. 1451–1458, Oct. 1998.

[18] Y. Ma and M. Pätzold, "Performance analysis of Alamouti coded OFDM systems over Rayleigh fading channels correlated in space and time," in *Proc. the 71st IEEE Vehicular Technology Conference, VTC2010-Spring, Taipei*, May 2010, pp. 1–6.

[19] A. Papoulis and S. U. Pillai, *Probability, Random Variables and Stochastic Processes*, 4th ed. New York: McGraw-Hill, 2002.

[20] B. O. Hogstad, C. A. Gutiérrez, M. Pätzold, and P. M. Crespo, "Classes of sum-of-cisoids processes and their statistics for the modeling and simulation of mobile fading channels," *EURASIP J. Wireless Commun. Netw.*, vol. 2013 (1), pp. 1–15, May 2013. doi: 10.1186/1687-1499-2013-125.